MATERIAL DEGRADATION MONITOR 2 (MDM2) MISSION: GROUND ANALYSIS RESULTS

Aki Goto and Yugo Kimoto

Japan Aerospace Exploration Agency (JAXA), 2-1-1 Sengen, Tsukuba, Ibaraki 305-8505, Japan, goto.aki@jaxa.jp

ABSTRACT

Material Degradation Monitor 2 (MDM2) mission is a material exposure experiment on Exposed Experiment Handrail Attachment Mechanism (ExHAM) attached to the International Space Station (ISS) Japan Experiment Module (JEM called Kibo) Exposed Facility. In this mission, sixteen material samples installed on the MDM2 sample holding part and fixed on the ExHAM, were exposed in the ISS orbit environment for about one year from May 26, 2015 to June 13, 2016, and then returned on the ground.

The material samples include an atomic oxygen (AO) monitor material, thermal control films (used as multilayer insulation (MLI) and optical solar reflector (OSR)), and wire cables. These samples are expected to be used in future satellites in a super low altitude (< 300 km), and the same as the samples installed on material degradation monitor (MDM), which is a mission sensor of Super Low Altitude Test Satellite (SLATS called TSUBAME), developed by JAXA and launched on December 23, 2017. Although MDM2 mission can not acquire the material degradation data in a super low altitude like MDM mission, it has the merit that the detailed analysis of the exposed samples can be performed after the samples return to the ground. The outcome obtained from MDM and MDM2 missions has a plan to be used for spacecraft design standards for future satellites in super low altitude, material developments, and ground test technologies.

This paper presents the ground analysis results of the MDM2 material samples.

1. INTRODUCTION

Earth observation with a satellite using in a super low altitude (< 300 km) is expected to increase the resolution of optical images and reduce the transmission power of observation sensors. In order to demonstrate the flight technology at super low altitude, JAXA developed Super Low Altitude Test Satellite: SLATS called TSUBAME and launched it on December 23, 2017[1-3]. In a very low altitude, the satellite receives about a thousand times air drag compared with the general satellite orbit altitude (about 600 to 800 km). Therefore, to maintain the altitude of the satellite, a large amount of propellant is required. Regarding SLATS, the high propellant efficiency of the ion thruster systems compensates to maintain the satellite altitude throughout the entire mission.

Meanwhile, one of the problems in the satellite mission in a low earth orbit (LEO) is the degradation of materials used on the satellite surface due to atomic oxygen (AO). AO is a neutral gas formed by dissociation of oxygen molecules by ultraviolet rays (UV) from the sun[4]. It collides with polymer materials such as thermal control films at the spacecraft rotating velocity, thereby oxidizing and eroding their surfaces. In addition, the reaction between AO and a polymer material lowers the functions of the materials such as the mechanical properties[5] and thermo-optical properties. Especially in a super low altitude, the density of AO is much higher than that in a general altitude[6], therefore the serious degradation of materials is concerned. For the success of the satellite mission in a super low altitude, it is required to evaluate materials using the ground-based AO irradiation test facility. However, reproducing the number of AO collisions with materials (AO fluences) in a super low altitude on the ground takes a huge amount of time, so it is not realistic.

To solve the problems of the material degradation due to AO in super low altitude, JAXA performed MDM[7] and MDM2 mission. MDM is one of the mission sensors of SLATS, and observes the degradation behaviors of the material samples in very low altitude using a CCD camera. There is no example of the image observation of the material degradation in an actual super low altitude environment, so MDM mission is the first attempt in the world. On the other hand, MDM2 is a material exposure experiment on the ISS using Exposed Experiment Handrail Attachment Mechanism (ExHAM)[8] developed by JAXA. In MDM2 mission, the material samples were exposed in the ISS orbit (about 400 km) altitude environment for about one year from May 26, 2015 to June 13, 2016, and then returned on the ground. Although MDM2 mission can not acquire the material degradation data in a super low altitude like MDM mission, it has the merit that the detailed analysis of the exposed samples can be performed after the samples return to the ground. The material samples exposed in MDM and MDM missions are mostly the same, and expected to be used in future satellites in super low altitude.

This paper presents the ground analysis results of the MDM2 material samples.

2. MDM2 MISSION

2.1 Sample holding part

Fig. 1 shows MDM2 sample holding part. The sample holding area is about 10 cm x 10 cm, and material samples are installed by some screws or an adhesive. This sample holding part was attached on the RAM face

(forward relative to ISS orbit) of ExHAM, where AO vertically collides with material samples (**Fig. 2**).

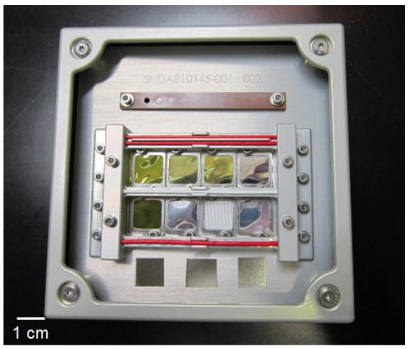

Fig. 1 MDM2 sample holding part (exposed face; before space exposure)

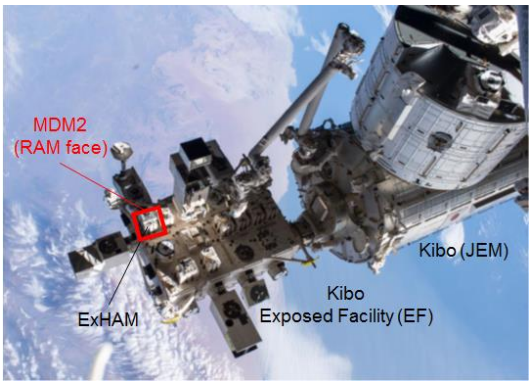

Fig. 2 Positions of ExHAM and MDM2 sample holding part on Kibo Exposed Facility (EF)

2.2 Material samples

Table 1 lists the material samples installed on MDM2 sample holding part and their applications. **Fig. 3** shows the positions of installed samples. Sixteen material samples include an AO monitoring material, films used for thermal control materials such as MLI, OSR, and wire cables. These samples are expected to be used in future satellites in super low altitude, and the same as the samples installed on MDM, which is a mission sensor of SLATS except for flexible-OSRs (installed position: 14-16). The exposure area of the film samples is about 1 cm x 1 cm.

Vespel® (installed position: 1), which is a bulk polyimide, was used as the AO monitoring material to determine the number of AO collisions with material samples, because its reaction yield to AO is already known as 3.00×10^{-24} cm^3/atom. It was adopted as an AO monitoring material in the past material exposure experiments performed by JAXA such as SM/SEED (SM: Russian Service Module, SEED: Space Environment Exposure Device)[8] and JEM/SEED (JEM: Japanese Experiment Module)[9].

AO protective (*SQ*) coated polyimide film (installed position: 2)[10] is a polyimide film (Upilex-R) coated and cured with a coating (*SQ* coating) composed mainly of silsesquioxane derivatives developed by JAXA. It is known that the silica layer formed by the reaction between the *SQ* coating layer and AO becomes a protective layer from AO. AO protective (polysiloxane block) polyimide film (BSF-30; installed positions: 3, 4) is a film developed by JAXA which itself has an AO protective performance and known that the silica layer formed by the reaction between the base film and AO becomes a protective layer from AO. One of them is coated with an UV shielding coating composed of cerium oxide (CeO_2; installed position: 4).

Three kinds of silvered fluorinated ethylene propylene films (FEP/Ag) were also selected (installed positions: 9, 11, 13), and one of them is coated with indium tin oxide (ITO; installed position: 13), which exhibits an AO protective performance. All silvered FEP samples have an Inconel® layer (thickness: 28 nm), which is a Ni alloy having an oxidation-resistant property, on the outside surface of the Ag face. Additionally, polyimide film (Kapton®) with ITO and Beta Cloth, which is a glass fiber fabric, were selected (installed positions: 10, 12).

Flexible-OSR is an OSR film mainly composed of polyetherimide (PEI) developed by JAXA (installed positions: 14-16). It has 5 layers such as ITO, CeO_2, PEI, Ag alloy called APC, and Inconel®. In MDM2 mission, three kinds of flexible-OSR manufactured under different conditions were selected and attached to the sample holding part with an acrylic adhesive.

Expanded polytetrafluoroethylene (PTFE) cables and an ETFE (tetrafluoroethylene-ethylene copolymer) cable are wire cables used for photovoltaic paddles.

2.3 Space exposure period

The MDM2 sample holding part was launched on April 15, 2015 by the Dragon SpX-6. It was fixed on ExHAM and exposed in the ISS orbit environment (altitude: about 400 km) for about one year from May 26, 2015 to June 13, 2016, and then returned to the ground by the Dragon SpX-9 on August 27, 2016.

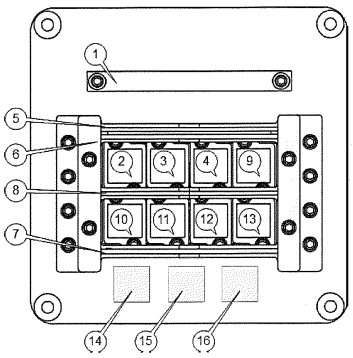

Fig. 3 Positions of installed material samples on MDM2 sample holding part

Table 1 MDM2 material samples

Installed position	Material sample	Application
1	Vespel®	AO monitor
2	AO protective (*SQ*) coating/polyimide film (Upilex-R) /Al [a)]	MLI
3	AO protective (polysiloxane block) polyimide film (BSF-30)/Al [b)]	
4	UV shielding coating (CeO_2)/AO protective polyimide film (BSF-30)/Al [a)]	
10	ITO coating/polyimide film (Kapton®)/Al [a)]	
12	Beta Cloth/Al [b)]	
5	Expanded PTFE cable (ϕ 1.18 mm)	Cable
6	Expanded PTFE cable (ϕ 1.35 mm)	
7	Expanded PTFE cable (ϕ 1.58 mm)	
8	ETFE cable	
9	FEP (1 mil [d)]) film/Ag [b)]	OSR
11	FEP (5 mil [d)]) film/Ag [b)]	
13	ITO coating/FEP (5 mil [d)]) film/Ag [a)]	
14, 15, 16	Flexible-OSR 263, 261, 213 [c)]	

a) Coating (exposed face)/base film/coating (back face)
b) Base film (exposed face)/coating (back face)
c) The numbers mean the manufacturing conditions of the flexible-OSRs.
d) Thickness of the FEP film

3. GROUND ANALYSIS

3.1 AO monitor

The mass loss of the Vespel® was measured by the micro-electronic balance XP6 (Mettler Toledo Co., Ltd.) to determine the number of AO collisions with material samples (AO fluence) by the equation (1).

$$F = \frac{\Delta m}{A \rho E_y} \quad (1)$$

F: Number of AO collision [atoms/cm^2]
Δm: Mass loss of the Vespel® [g]
A: Exposed area of the Vespel® (3.21 cm^2)
ρ: Density of the Vespel® (1.43 g/cm^3)
E_y: Reaction yield to AO of the Vespel® (3.00×10^{-24} cm^3/atom)

3.2 Films

Regarding film samples except for the flexible-OSRs, their mass losses were measured by the method shown above. And, regarding all film samples, their thermos-optical properties such as solar absorptance (α_s) and the normal infrared emittance (ε_N) were measured before and after exposure by U-4100 (Hitach High-Technologies Co., Ltd.) and TESA2000 (AZ Technology Co., Ltd.), respectively. The α_s and ε_N of the flexible-OSR were measured with the sample holding part composed of Al alloy.

3.2.1 *SQ* coated polyimide film

In order to evaluate the reaction between the *SQ* coating and AO, the cross section of the exposed and pristine *SQ* coated polyimide film were observed by the scanning transmission electron microscope (STEM; JEM-ARM200F (JEOL Co., Ltd.)), and their composition spatial-distributions were analysed by the energy dispersive X-ray spectrometry (EDX; JED2300 (JEOL Co., Ltd.)). For the STEM sample preparation, the focused ion beam (FIB) technique (SMI3200SE (SIINT Inc.), FB-2000A-2 (Hitachi Co., Ltd.), Strata 400S (FEI Co., Ltd.)). And, some cracks formed on the surface of the *SQ* coated polyimide film in the space exposure were observed by the digital microscope VHX-900 (Keyence Co., Ltd.).

3.2.2 Silvered FEP

In order to investigate the invasion route of AO related to the oxidation phenomenon of the Ag layer, a ground AO irradiation test was performed by using the Combined Space Effect Test Facility at JAXA Tsukuba Space Center. The AO generation is based on a laser detonation phenomenon. The AO velocity was controlled to about 8 km/s.

The FEP (1 mil)/Ag and FEP (5 mil) were set on an engineering model (EM) of the MDM sample holding part or a specific sample holder, which is usually used in the ground AO irradiation test, and irradiated with AO. The AO fluence, which was estimated from the mass loss of AO monitors (Kapton®), was 5.2 x 10^{20} atoms/cm^2. The AO irradiation using the EM seems to reproduce the AO exposure environment in MDM2 mission to some extent. When using the EM or the actual MDM2 sample holding part, there is a little space behind the film sample, so there is a possibility that AO invades there. On the other hand, the sample holder can shield the back face and the edge of the film sample, therefore it seems that the AO-invasion into the backside of the film sample when using it.

The element compositions and its spatial-distribution of the Ag faces of the pristine and the irradiated silvered FEP samples were analysed by the X-ray photoelectron spectrometer (XPS; K-Alpha (Thermo Scientific Co.,

Ltd.)) and the electron probe micro analyser (EPMA; EPMA-1600 (Shimazu Co., Ltd.), respectively. And, the Ag density in the Inconel® layer of the Ag (back) faces of the pristine silvered FEPs was analysed by the secondary ion mass spectrometry (D-SIMS; PHI ADEPT1010 (ULVAC-PHI Co., Ltd.)

3.3 Cables

The cross-sections of the wire cable samples before and after exposure were observed by the digital microscope VHX-900 and measured the reduction of the wire cable covering materials related to the space exposure.

4. RESULT AND DISCUSSION

4.1 AO monitor

The mass loss of the Vespel® in the space exposure for about one year was 2.83 x 10^{-2} g. The AO fluence determined by this mass loss and the equation (1) was 2.0 x 10^{21} atoms/cm^2. The AO fluence in the MDM2 exposure period (May 26, 2015 to June 13, 2016) calculated by JAXA Space Environment & Effects System (SEES)[11] is 1.47 x 10^{21} atoms/cm^2 (using NRLMSISE-00 model[6]; orbit data: the ISS orbit, version of solar radio-wave intensity and geomagnetic activity: Ver. 81 (Feb, 2017), setting of solar radio-wave intensity and geomagnetic activity: Mean). The AO fluence calculated by using the environment model was in agreement with that measured by the mass loss of the Vespel® within 30%. This result suggests that the environment model has some validity.

4.2 Films

4.2.1 External appearance

Table 2 shows the external appearances of the film samples before and after exposure. For the *SQ* coated polyimide film, the BSF-30, and the Beta Cloth, there was a little discoloration of the exposed face due to the space exposure. Regarding the silvered FEPs, the Ag (back) face partially turned black in the exposure, which seems that Ag was oxidized by AO (**Fig. 4**). Especially for the FEP (1 mil)/Ag, the oxidization of the Ag layer was remarkable, and a part of the Ag layer was peeled off (**Fig. 4a**). For the UV shielding coated BSF-30, the ITO coated polyimide film, and the flexible-OSRs, there was no visible change of the exposed face in the exposure.

By comparing the external appearance of the BSF-30 and the UV shielding coated BSF-30, it was qualitatively confirmed that the UV shielding coating (CeO_2) suppresses discoloration of the film surface due to UV. The factors related to the oxidation of Ag layer of the silvered FEPs are discussed in **Section 4.2.5**.

Table 2 External appearances of the film samples before and after exposure (exposed faces)

No. [a)]	Material sample	Before exposure	After exposure
2	*SQ* coating/ polyimide film/Al		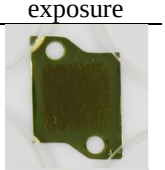
3	BSF-30/Al		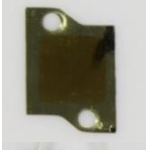
4	UV shielding coating/ BSF-30/Al	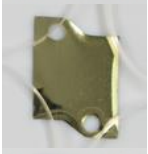	
9	FEP (1 mil) film/Ag		
10	ITO coating/ polyimide film /Al		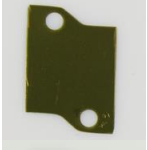
11	FEP (5 mil) film/Ag		
12	Beta Cloth/Al	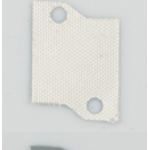	
13	ITO coating/ FEP (5 mil) film/Ag		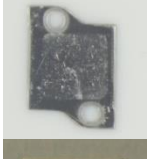
14	Flexible-OSR 263	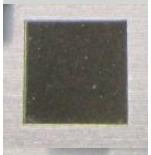	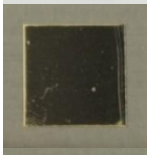
15	Flexible-OSR 261	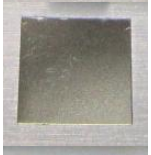	
16	Flexible-OSR 213		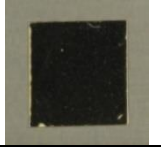

a) The number means the installed position of each film sample.

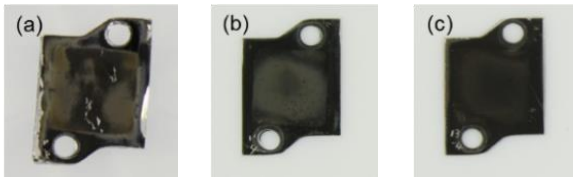

Fig. 4 Back faces (Ag faces) of the silvered FEP films after exposure: (a) FEP (1 mil) film/Ag (installed position: 9), (b) FEP (5 mil) film/Ag (installed position: 11), (c) ITO/FEP (5 mil)/Ag (installed position: 13)

4.2.2 Mass loss

Table 3 lists the mass loss and mass change ratio of the film samples in the space exposure. Regarding the *SQ* coated polyimide film, the BSF-30, the UV shielding coated BSF-30, the ITO coated polyimide film, the FEP (5 mil)/Ag, and the ITO coated FEP (5 mil)/Ag, there was no significant mass change due to the exposure. It suggests that no serious erosion of the surface of these films by AO occurred.

Meanwhile, the mass of the FEP (1 mil)/Ag decreased by 5%. The contribution ratio of the FEP's erosion by AO and the Ag layer's peeled-off to this mass loss can not be clearly identified, but when considering the mass loss of the FEP (5 mil)/Ag, it seems that the mass loss of the FEP (1 mil)/Ag is mainly due to the Ag layer's peeled-off.

Table 3 Mass loss and mass change ratio of the film samples in the space exposure

No.[a)]	Material sample	Mass loss [mg/cm^2]	Mass change ratio [b)]
2	*SQ* coating/ polyimide film/Al	0.08	0.99
3	BSF-30/Al	0.02	1.00
4	UV shielding coating/ BSF-30/Al	-0.01	1.00
9	FEP (1 mil) film/Ag	0.56	0.95
10	ITO coating/ polyimide film /Al	0.08	0.99
11	FEP (5 mil) film/Ag	0.52	0.99
12	Beta Cloth/Al	0.45	0.99
13	ITO coating/ FEP (5 mil) film/Ag	0.035	1.00

a) The number means the installed position of each film sample.
b) Mass ratio after to before exposure

4.2.3 Thermo-optical property

Table 4, 5 list the solar absorptance (α_s) and normal infrared emittance before and after the exposure, and their changes of the film samples, respectively. For the *SQ* coated polyimide film, the UV shielding coated BSF-30, the ITO coated polyimide film, the Beta Cloth, and the flexible-OSRs, the change of the solar absorptance and normal infrared emittance in the exposure was a little, so considering this and the results of the mass loss (**Table 3**), it was demonstrated that these samples have high durability in the ISS orbit environment.

The solar absorptance of the BSF-30 after the exposure was about 30% higher than before. This change is considered due to the discoloration of the surface of the BSF-30 based on the reaction with UV. In the case that the increase in solar absorptance of the BSF-30 becomes a problem in the thermal design of a satellite, it can be said that the application of the UV shielding coating is desirable. Regarding the silvered FEPs, the solar absorptances after the exposure were 70 – 330 % higher than before. One of the factors related to the solar absorptance changes seems to be the oxidization of the Ag layer in the exposure. The solar absorptance of a silvered FEP is known to depend on mainly the light reflection property of the Ag layer. During this space exposure, it is considered that the Ag layer of the silvered FEP was oxidized by an AO invasion, its light reflection property was lowered, and then the solar absorptance of the film increased. The AO invasion route and the factor related to the serious oxidization of the Ag layer of the FEP (1 mil)/Ag are discussed in **Section 4.2.5**.

Table 4 Solar absorptance (α_s) before and after exposure, and its change ratio of the film samples

No.[a)]	Material sample	α_s before [b)]	α_s after [b)]	Change ratio [c)]
2	*SQ* coating/ polyimide film/Al	0.34	0.38	1.1
3	BSF-30/Al	0.27	0.34	1.3
4	UV shielding coating/ BSF-30/Al	0.23	0.24	1.0
9	FEP (1 mil) film/Ag	0.07	0.30	4.3
10	ITO coating/ polyimide film /Al	0.37	0.37	1.0
11	FEP (5 mil) film/Ag	0.07	0.12	1.7
12	Beta Cloth/Al	0.39	0.43	1.1
13	ITO coating/ FEP (5 mil) film/Ag	0.08	0.17	2.1
14	Flexible-OSR 263	0.18	0.19	1.1
15	Flexible-OSR 261	0.19	0.19	1.0
16	Flexible-OSR 213	0.18	0.19	1.1

a) The number means the installed position of each film sample.
b) Before or after exposure
c) α_s ratio after to before exposure

Table 5 Normal infrared emittance (ε_N) before and after exposure, and its change ratio of the film samples

No.[a)]	Material sample	ε_N before [b)]	ε_N after [b)]	Change ratio [c)]
2	*SQ* coating/ polyimide film/Al	0.80	0.77	0.96
3	BSF-30/Al	0.82	0.82	1.0
4	UV shielding coating/ BSF-30/Al	0.83	0.83	1.0
9	FEP (1 mil) film/Ag	0.57	0.60	1.1
10	ITO coating/ polyimide film /Al	0.84	0.85	1.0
11	FEP (5 mil) film/Ag	0.86	0.85	0.99
12	Beta Cloth/Al	0.96	0.96	1.0
13	ITO coating/ FEP (5 mil) film/Ag	0.86	0.86	1.0
14	Flexible-OSR 263	0.88	0.89	1.0
15	Flexible-OSR 261	0.85	0.90	1.1
16	Flexible-OSR 213	0.86	0.87	1.0

a) The number means the installed position of each film sample.
b) Before or after exposure
c) ε_N ratio after to before exposure

4.2.4 *SQ* coated polyimide film

In order to evaluate the reaction and its progress between the *SQ* coating and AO in the exposure, the cross section of the exposed and pristine *SQ* coated polyimide film was observed by the STEM. **Fig. 5** shows the STEM images. Before the exposure, the thickness of the *SQ* coating was 1.1 μm (**Fig. 5a**). And, after the exposure, the thickness of the coating was 0.54 μm, that is, the thickness decreased due to the exposure, and two kinds of layers were observed on the coating layer (formed layer A and B; **Fig. 5b, c**) The thickness of the formed layer A and B was 30 and 80 nm, respectively. The element composition of the formed layer A and B was analysed by the EDX (**Table 6**). The formed layer A was composed of 31% Si and 66% O, which means the layer consists mainly of SiO_2 (silica). And, the formed layer B was composed of 26% Si, 64% O, and 10% C. This composition indicates the layer consists of the mixture of silica (SiO_x) and some organic components. The high purity silica was found to be formed as closer to the exposed surface of the film.

These results obtained by the STEM and the EDX suggest that the reaction between the *SQ* coating, composed mainly of silsesquioxane derivatives, and AO gives the dissociation of some organic units and the formation of a silica layer. The formed silica layer plays a role of a protective layer from AO, therefore we could demonstrate the AO protective capability of the *SQ* coating in the scale from several tens to several hundred nm.

However, for the exposed *SQ* coated polyimide film, some cracks with a few μm scale were observed on the exposure surface. **Fig. 6** shows the digital microscope image of the surface of the exposed *SQ* coated polyimide films and the STEM image of the cross-section of its crack position. The depth of a formed crack was about 6 μm, and the crack was found to reach the polyimide layer (**Fig. 6b**). And, it was confirmed that another crack also reached the polyimide layer. The erosion of a polyimide film by AO may progress from such crack positions. Our future task is to investigate the factors related to the formation of cracks, and the influence of cracks on the AO protective performance of the film.

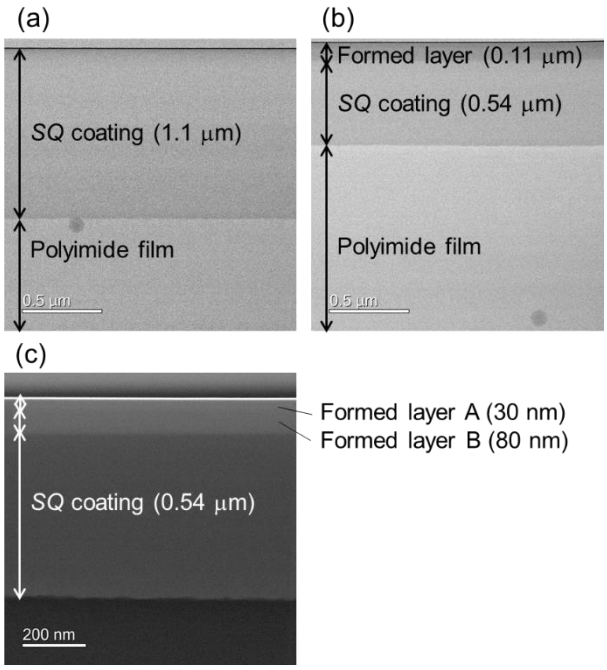

Fig. 5 STEM images of the cross-section of the *SQ* coated polyimide films before (a) and after (b, c) exposure: (a), (b) BF (Bright Field) images, (c) HAADF (High Angle Annular Dark Field) image (acceleration voltage: 200 kV)

Table 6 Element compositions of the cross-section of the *SQ* coated polyimide film after exposure analysed by the EDX

	Element compositions analysed by the EDX [atom%]			
	C	N	O	Si
Formed layer A	3.4	-	66.1	30.5
Formed layer B	10.0	-	63.5	26.4
SQ coating	39.1	0.63	43.8	16.4

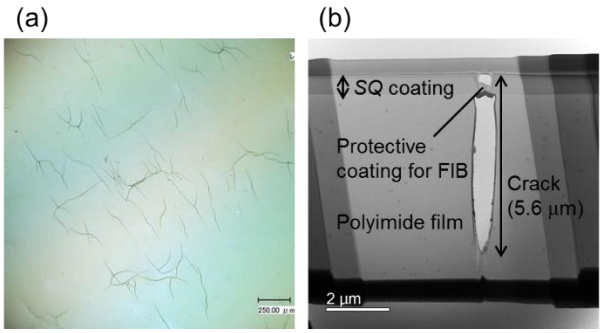

Fig. 6 (a) Digital microscope image of the surface of the *SQ* coated polyimide films after exposure, (b) BF-STEM image of the cross-section of the *SQ* coated polyimide films (crack position) after exposure (acceleration voltage: 200 kV)

4.2.5 Silvered FEP

In order to investigate the invasion route of AO related to the oxidation phenomenon of the Ag layer, the FEP (1 mil)/Ag and the FEP (5 mil)/Ag were irradiated with AO using the ground AO irradiation test facility on the engineering model (EM) of the MDM sample holding part, which enables to reproduce the AO exposure environment in MDM2 mission to some extent, or a specific sample holder, which is usually used in the ground AO irradiation test. And, for the pristine and AO-irradiated silvered FEPs, the element compositions and its spatial-distribution were analysed by the XPS and the EPMA.

Fig. 7, **8** show the depth profiles of the element compositions of the Ag (back) faces of the FEP (1 mil)/Ag and the FEP (5 mil)/Ag obtained by the XPS, respectively. These depth profiles suggest that all films have an Inconel® layer, which has an oxidation-resistant property, with a few tens nm thickness regardless of the AO irradiation and the thickness of FEP film. And, for the AO irradiated silvered FEPs on the EM, the Ag was found to be penetrated through the Inconel® layer (**Fig. 7b, 8b**). On the other hand, for the AO irradiated samples on the sample holder, the penetration of Ag was not observed (**Fig. 7c, 8c**).

Table 7 shows the backscattered electron (BSE) composition images of the Ag (back) faces of the pristine and the AO-irradiated silvered FEPs obtained by the EPMA. The composition of the Ag face of the pristine samples in the observation area (about 100 µm x 75 µm) was homogeneous. The BSE images of the Ag face of the AO-irradiated samples on the EM have some relatively dark spots, and the number of such spots was much larger in the image of the FEP (1 mil)/Ag than in that of the FEP (5 mil)/Ag. And, the number of the dark spots was larger in the image of the AO-irradiated samples on the EM than in the irradiated samples on the sample stage. In BSE images, a relatively dark position, where the number of detected backscattered-electrons is smaller, means consisting of lighter elements. Therefore, the dark spots shown in the BSF images of the Ag face of the AO-irradiated samples seems to be the spots where the Ag was oxidised

By the XPS and the EPMA analysis, it was found that the Ag penetration through the Inconel® layer and the Ag oxidization due to the AO irradiation, shown when using the EM, were suppressed when using the sample holder. This result suggests that the oxidization phenomenon of the Ag layer of the silvered FEP samples shown in this space exposure was due to the AO invasion into the Ag layer from the backside or the edge of the film.

As a factor related to the serious oxidation of the Ag layer of the FEP (1 mil)/Ag, we think that the Inconel® layer of the pristine FEP (1 mil)/Ag contains Ag. **Fig. 9** shows the depth profiles of the Ag density in Ni of the pristine FEP (1 mil)/Ag and the pristine FEP (5 mil)/Ag obtained by the SIMS. These profiles indicate that the Ag density in the Inconel® layer of the pristine FEP (1 mil)/Ag is up to ten times higher than that of the pristine FEP (5 mil)/Ag. Therefore, we think, since much Ag in the Inconel® layer of the FEP (1 mil)/Ag reacted with the invading AO in the exposure, the serious oxidation of the Ag layer was observed.

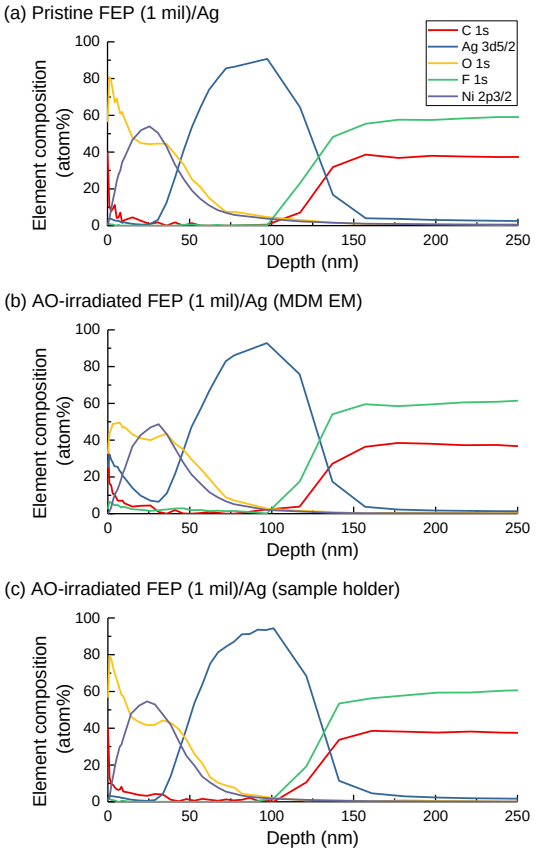

Fig. 7 Depth profiles of the element compositions of the Ag (back) faces of the FEP (1 mil)/Ag (Ag face) samples obtained by the XPS: (a) pristine, (b) AO-irradiated on the MDM-EM, (c) AO-irradiated on the sample holder (depth: SiO_2 conversion; Etching: Ar beam (3 keV))

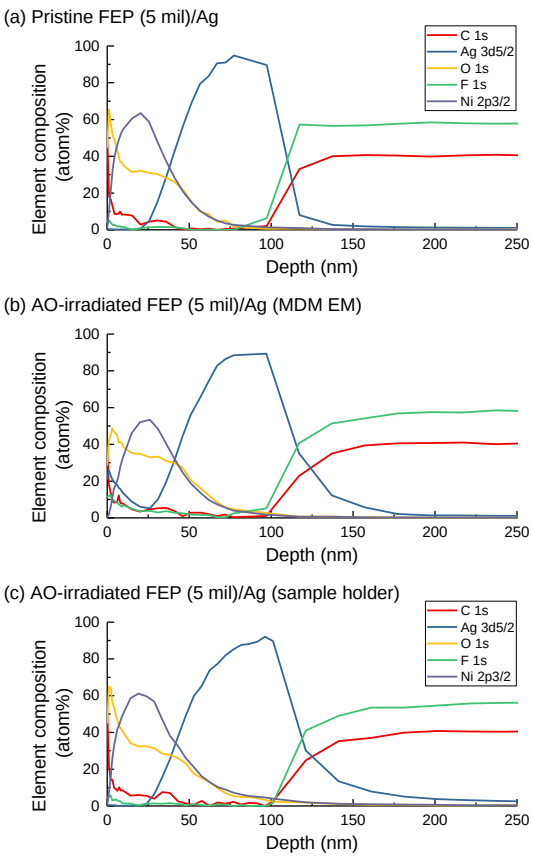

Fig. 8 Depth profiles of the element compositions of the Ag (back) faces of the FEP (5 mil)/Ag (Ag face) samples obtained by the XPS: (a) pristine, (b) AO-irradiated on the MDM-EM, (c) AO-irradiated on the sample holder (depth: SiO_2 conversion; Etching: Ar beam (3 keV))

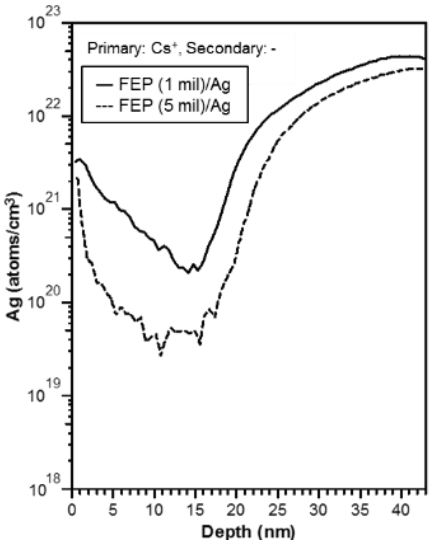

Fig. 9 Depth profiles of the Ag density in Ni of the pristine FEP (1 mil)/Ag and the pristine FEP (5 mil)/Ag obtained by the SIMS (Ni standard sample was used for the quantification; primary ion: Cs^+ (2.0 kV))

Table 7 Backscattered electron (BSE) composition images of the Ag (back) faces of the pristine and the AO-irradiated silvered FEP samples obtained by the EPMA (scale bars: 10 μm)

	Ag (back) face	
	FEP (1 mil)/Ag	FEP (5 mil)/Ag
Pristine	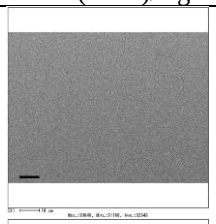	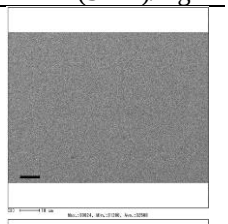
AO-irradiated (using the MDM EM)	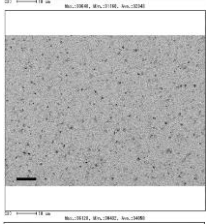	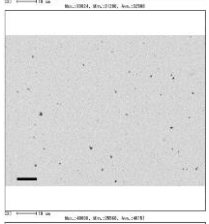
AO-irradiated (using the sample holder)	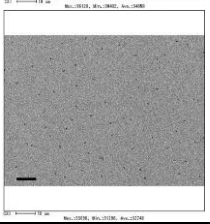	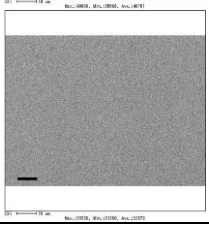

Considering the results shown above, we think that no serious oxidation of Ag layer of silvered FEP occurs in the actual satellite mission because the silvered FEP is generally attached to a satellite with an adhesive, and the AO invasion into the backside of the film hardly occurs. However, when using a silvered FEP with perforation, we think that it is desirable to evaluate the AO invasion from the perforation.

4.3 Cables

Table 8 shows the digital microscope images of the cross-section of the wire cables before and after the exposure. Regarding all wire cables, there was no significant reduction of the thickness of the wire cable covering material. Therefore, we found that the covering materials have the durability against AO in the ISS orbit environment.

5. CONCLUSION

In this paper, we showed the ground analysis results of the exposure samples in MDM2 mission. These samples were exposed on the RAM face of ExHAM in the ISS orbit environment for about one year (from May 26, 2015 to June 13, 2016), and then returned on the ground. As a result, regarding the *SQ* coated polyimide film, the UV shielding coated BSF-30, the ITO coated polyimide film, the Beta Cloth, the flexible-OSRs, and

the wire cables, it was demonstrated that these materials have high durability especially against AO in the ISS orbit environment. And, the UV shielding effect of the CeO_2 coating was qualitatively confirmed.

For the *SQ* coated polyimide film, it was confirmed that the AO protective layer consisting mainly of silica was formed by the reaction between the *SQ* coating and AO in the exposure. And, regarding the silvered FEP, the factors related to the oxidation of the Ag layer in the exposure were investigated by performing the ground AO-irradiation tests. It suggested that the oxidization phenomenon of the Ag layer shown in this exposure was due to the AO invasion into the Ag layer from the backside or the edge of the film.

The outcome obtained from MDM and MDM2 missions plans to be used for spacecraft design standards for future satellites in super low altitude, material developments, and ground test technologies.

Table 8 Digital microscope images of the cross-section of the wire cables before and after exposure (scale bars: 200 μm)

No.[a)]	Material sample	Before exposure [b)]	After exposure [b)]
5	Expanded PTFE cable (ϕ 1.18 mm)		
6	Expanded PTFE cable (ϕ 1.35 mm)	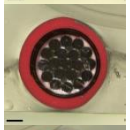	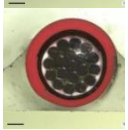
7	Expanded PTFE cable (ϕ 1.58 mm)		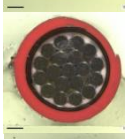
8	ETFE cable		

a) The number means the installed position of each cable sample.
b) The observation positions of the samples before and after exposure are different.

REFERENCES

1. H. Hoshino et al., "SLATS and Future Prospect-New viewpoints for Earth Observation -", Proc. of 31st ISTS, 2017-n-09, 2017.
2. H. Kawasaki et al., "Interim Report of Super Low Altitude Satellite Operation", Proc. of IGARSS, 2018.
3. M. Sasaki, "Mission for Super-Low Earth Orbit", Space Research Today, No.198, COSPAR's Information Bulletin, No.198, pp.10-18, 2017.
4. T. K. Minton et al., "Dynamics of Atomic Oxygen Induced Polymer Degradation In Low Earth Orbit", Chemical Dynamics In Extreme Environments, edited by R. A. Dressler, Advanced Series in Physical Chemistry, Vol. 11, 2001.
5. H. Shimamura, et al., "Investigation of degradation mechanisms in mechanical properties of polyimide films exposed to a low earth orbit environment", Polym. Degrad. Stab. 95, pp.21-33, 2010.
6. J. M. Picone et al., "NRLMSISE-00 empirical model of the atmosphere: Statistical comparisons and scientific issues", J. Geophys. Res. Space. Phys. 107, pp.1468, 2002.
7. Y. Kimoto et al., "Analysis of First Data from Atomic Oxygen Monitor System onboard SLATS", Proc. of 14th ISMSE, 2018.
8. Y. Kimoto et al., "Passive Space-Environment-Effect Measurement on the International Space Station", J. Spacecraft Rockets, 46, pp.22-27, 2009.
9. J. Kleimen, "Protection of Materials and Structures from the Space Environment", Astrophys. Space. Sci. Proceedings, 32, pp.73-82, 2013.
10. Y. Kimoto et al., "Development of Space-Qualified Photocurable-Silsesquioxane-Coated Polyimide Films", J. Spacecraft Rockets, 2016.
11. JAXA Space Environment & Effects System: SEES, http://seesproxy.tksc.jaxa.jp/fw/dfw/SEES/Japanese/Top/top_j.shtml